ELSEVIER

Marine Geology 189 (2002) 197–214

MARINE GEOLOGY
INTERNATIONAL JOURNAL OF MARINE GEOLOGY, GEOCHEMISTRY AND GEOPHYSICS

www.elsevier.com/locate/margeo

Fluctuation of biogenic and abiogenic sedimentation on the Shatsky Rise in the western North Pacific during the late Quaternary[1]

Lena Maeda [a,*], Hodaka Kawahata [a,b], Masato Nohara [b]

[a] *Graduate School of Science, Tohoku University, Aoba, Sendai 980-8578, Japan*
[b] *National Institute of Advanced Industrial Science and Technology (AIST), Tsukuba-higashi 1-1-1, Ibaraki 305-8567, Japan*

Received 20 February 2001; accepted 23 May 2002

Abstract

Sedimentation of biogenic and abiogenic components was studied in cores NGC108 (36°36.85′N, 158°20.90′E; water depth 3390 m) and S2612 (32°19.84′N, 157°51.00′E; water depth of 2612 m) from the Shatsky Rise to understand fluctuations in primary productivity and abiogenic sedimentation in the mid-latitude of the western North Pacific during the late Quaternary. The mean $C_{Organic}/N$ atomic ratio of 6.0–7.8 in both cores indicates that organic matter is mainly marine in origin. Organic carbon is positively correlated with biogenic opal in core NGC108 in contrast to a weak correlation in core S2612. Although the maxima of paleoproductivity estimates in both cores generally occur during glacial times, the paleoproductivity estimates, biogenic opal/carbonate ratios and the $C_{Organic}/C_{Carbonate}$ ratios have always been higher in core NGC108 than in core S2612 during the last 180 kyr, suggesting that the surface water at site NGC108 could have been influenced more by Subarctic water mass than at site S2612. However, the opal/carbonate ratio in core S2612 remains fairly constant relative to that in core NGC108, which might mean that the transition zone between Subarctic and Central water was narrower in latitude in at the oxygen isotope stage (OIS) 2/3 boundary, OIS 4 and OIS 6. Sedimentation of 13 inorganic elements has been measured in both cores. These elements are classified into four groups based on correlation between each element in content: (1) terrigenous components (Al, Ti, Fe), (2) biogenic calcareous material (Ca, Sr), (3) biogenic-scavenged elements (Mg, Zn, Cr, Be), and (4) the other elements (Mn, Ba, Cu, Ni). The terrigenous mass accumulation rates were elevated in OIS 2, 3 and 4 and late OIS 6 in core NGC108 while they were higher in early OIS 1, OIS 2, 4 and 6 in core S2612. MnO_2 and Ba might be redistributed during the sub-surface reduced condition. Especially precipitation of particle-reactive Be, which could be accelerated by both enhanced terrigenous input and biogenic vertical transport, has fluctuated largely in response to climatic change because of its short residence time (on the order of the oceanic mixing time).

Keywords: primary productivity; carbon cycle; inorganic geochemistry; mid-latitude; western North Pacific; the late Quaternary

[1] **Background data set**[2]
[2] http://www.elsevier.com/locate/margeo

* Corresponding author. Tel./Fax: +81-298-54-3765.
E-mail addresses: l.maeda@aist.go.jp (L. Maeda), h.kawahata@aist.go.jp (H. Kawahata).

0025-3227/02/$ – see front matter
PII: S0025-3227(02)00405-X

1. Introduction

The middle latitude area of the western North Pacific is sensitive to climatic change because it is located under the northern westerly wind system and in a transition zone between Subarctic Pacific Waters and Western North Central Water (Thompson and Shackleton, 1980; Thompson, 1981; Sancetta and Silvestir, 1986; Haug et al., 1995; Thunell and Mortyn, 1995). The Shatsky Rise is the only broad topographic plateau on the 4–5-km-deep abyssal seafloor in the western North Pacific and therefore the sediments have recorded both marine and terrestrial environmental changes (e.g., Maiya et al., 1976; Hovan et al., 1989; Ohkushi et al., 2000). Especially, regarding marine environments, the sea surface temperature, nutrient concentrations and primary productivity are sharply changed in the transition zone. For example, the Subarctic water mass shows higher primary productivity with higher biogenic opal flux in sinking particles, which could reduce PCO_2 in the surface water during the late spring (Kawahata et al., 1998a). In contrast, the Central (Subtropical) water mass is characterized by oligotrophic condition, which corresponds to a low primary productivity due to the permanent thermocline in the surface water. Regions in the Kuroshio Extension show steep gradients in biological fluxes and composition, and their latitudinal position would have shifted with global climatic change during the late Quaternary (Thompson and Shackleton, 1980).

On the other hand, land-derived materials are significant components of many marine sediments, and wind is known to be an important agent for transporting this continental material to the world ocean (e.g., Windom, 1975; Johnson, 1979; Janecek and Rea, 1985). The tiny dust particles are removed quickly, at hundreds of meters per day, from the surface ocean by large amorphous aggregates and fecal pellet transport (Honjo et al., 1982). It is well known that these eolian inputs have fluctuated at mid-latitude during the late Quaternary (e.g., Sarnthein et al., 1981, 1982; Dersch and Stein, 1994; Hovan et al., 1991; Hesse, 1994; Kawahata et al., 2000).

In order to improve our current understanding of sedimentation variability of biogenic and abiogenic components affected by climatic change, some useful records can be obtained from the western North Pacific. Therefore, we document changes in sedimentation of carbonate, organic carbon (OC), biogenic opal and inorganic elements during the late Quaternary on the Shatsky Rise. Then we evaluate the past productivity and discuss the fluctuation of abiogenic sedimentation in the mid-latitude of the western Pacific during the late Quaternary.

2. Study area and sediment sample

2.1. Study area

Westerlies stand between cold and warm atmospheres. Western North Pacific surface water is divided into Subarctic Pacific Water and Western North Central Water (Tomczak and Godfrey, 1994). The former is characterized by the existence of spring bloom caused by mixed layer development associated with thermocline disappearing in winter (Thompson, 1981). The latter consists of warm and saline water and features a permanent thermocline with a thick mixed layer (Thompson, 1981). Between these water masses, a transition zone is formed where the Kuroshio Extension flows eastward. Steep temperature, salinity and nutrient gradients are observed in the transition zone (Stommel and Yoshida, 1972; Joyce, 1987; Levitus et al., 1993; LEVITUS94; Kawahata et al., 1998a).

Sediment trap experiments across the transect at 175°E (Fig. 1) demonstrated that annual mean organic matter (OM) fluxes increased from the Western North Central Water to the Subarctic Pacific Water. Mean biogenic opal flux showed a similar latitudinal profile, but increased markedly from 34°N to 46°N. Therefore, biogenic opal/carbonate ratios in annual mean fluxes showed a steep gradient in the transition zone, under which the Shatsky Rise is located. It has an area of 750 000 km^2, extends over 1300 km trending northeast, and consists of three plateaus rising to depths of 3.5–2.5 km. Observation of a regional geomagnetic field suggests that the rise was

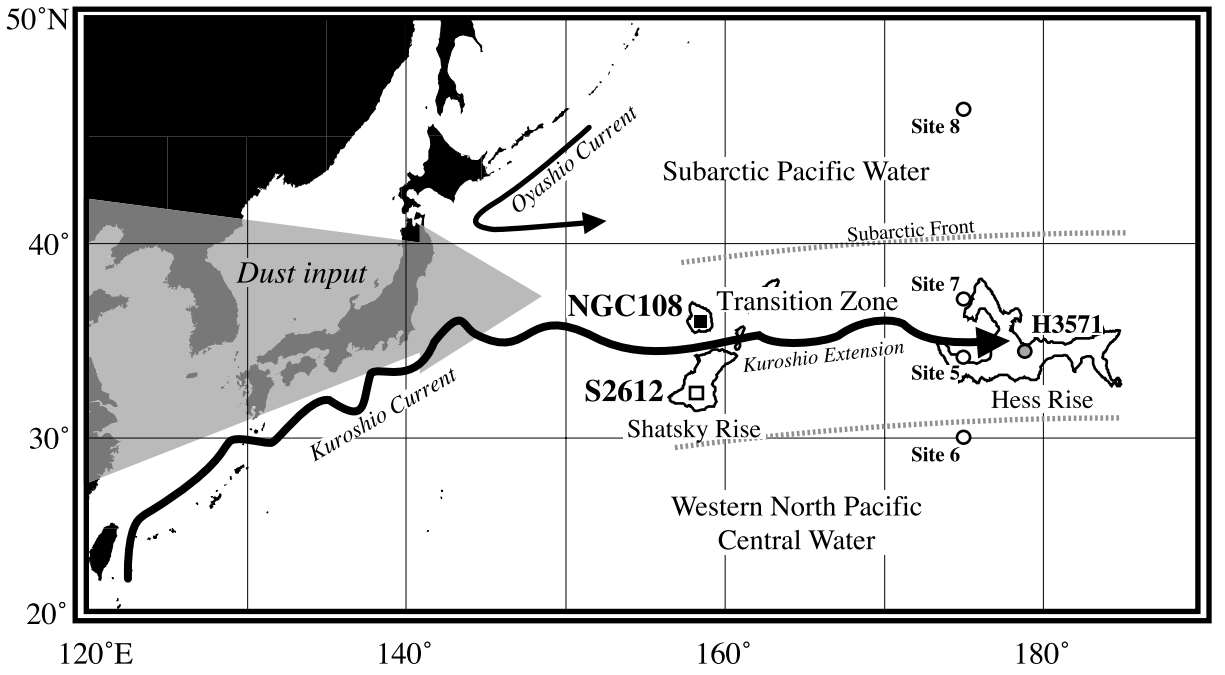

Fig. 1. Location of cores NGC108 and S2612 in the western North Pacific. The shaded circle indicates the location of core H3571 (see Kawahata et al., 2000). The path of the Kuroshio Extension is based on Mizuno and White (1983). The shaded arrow indicates a dust input pattern in spring based on the model of Navy Aerosol Analysis and Prediction System (http://www.nrlmry.navy.mil/aerosol/).

formed by a magmatic pulse on a hot-spot triple-junction intersection between the Late Jurassic and the Early Cretaceous (Nakanishi et al., 1989). The calcite compensation and lysocline depths in this area are estimated to be around 4.4 km and 3.2 km, respectively (Berger et al., 1976; Chen et al., 1988).

2.2. Core NGC108

The gravity core NGC108 was retrieved from the northwest plateau (36°36.85′N, 158°20.90′E; water depth 3390 m) during the NH95-1 cruise of the R/V *Hakurei-maru* under the Northwest Pacific Carbon Cycle Study (NOPACCS) program (Fig. 1). The total length of the sediment core is 645 cm, which is mainly composed of gray to olive gray silica-rich calcareous nannofossil ooze intercalated with two ash layers at 328–331 cm and 331–332 cm (Ioka et al., 1997). For this study, 86 samples for $\delta^{18}O$ isotopic analyses were taken at approximately 8-cm intervals, giving an average temporal sample interval of around 2.3 kyr.

2.3. Core S2612

A sedimentary core (S2612) of 329 cm length was collected from a water depth of 2612 m at 32°19.84′N, 157°51.00′E (Fig. 1). The core consists of dull yellowish brown oxidized calcareous nannofossil ooze at the top 12 cm and gray bioturbated calcareous ooze intercalated with a volcanic ash layer at 249 to 251 cm (Kawahata et al., 1999).

3. Analytical procedure

Separate samples were taken for chemical and foraminiferal isotopic analyses. Sediment aliquots for chemistry were frozen on board and kept at −20°C prior to analysis in a land-based laboratory. They were crushed to fine powder after drying

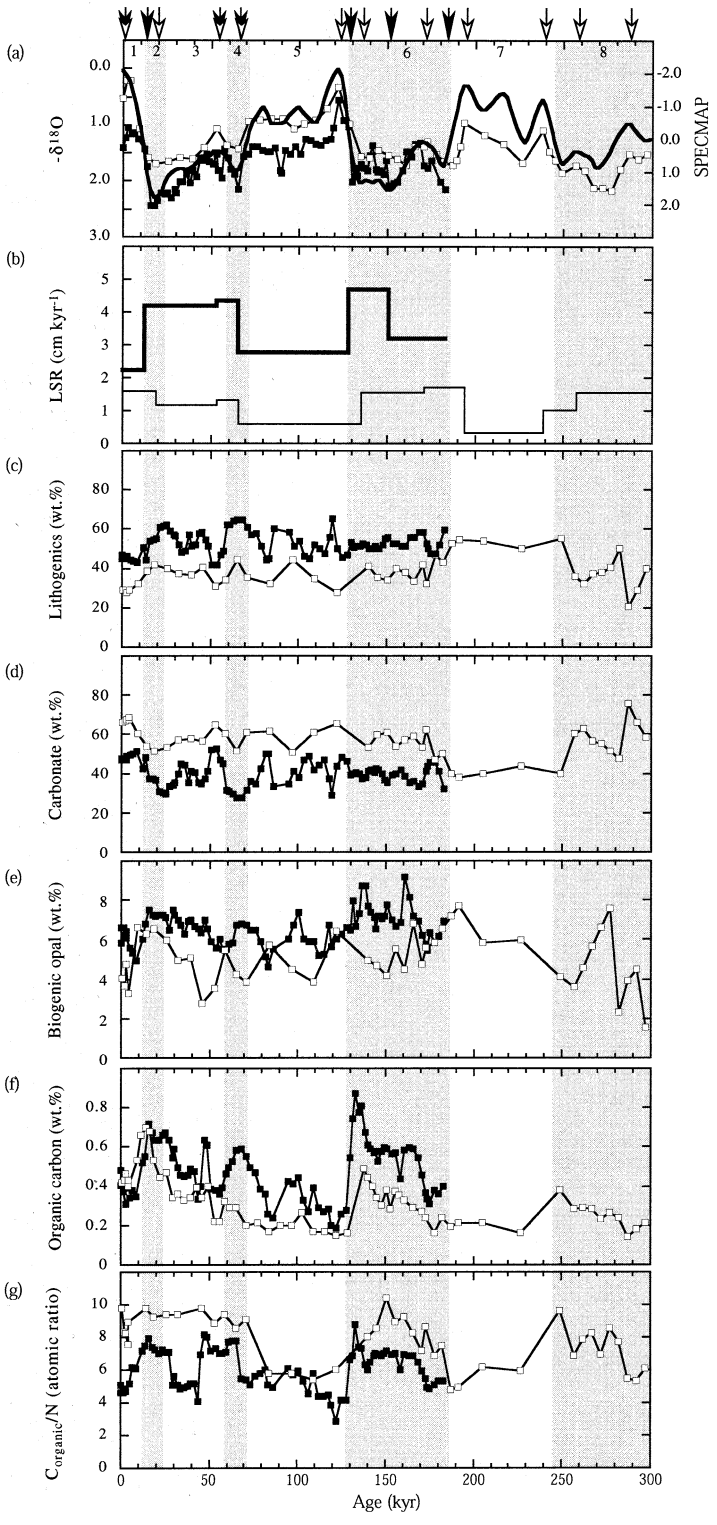
(a)
-δ18O
SPECMAP
1
2
3
4
5
6
7
8
(b)
LSR (cm kyr-1)
(c)
Lithogenics (wt.%)
(d)
Carbonate (wt.%)
(e)
Biogenic opal (wt.%)
(f)
Organic carbon (wt.%)
(g)
Corganic/N (atomic ratio)
Age (kyr)

at 40–50°C, and split into several subsamples for analyses.

Full details of the analytical procedure for total carbon, OC, and total nitrogen contents have been described elsewhere (Kawahata and Eguchi, 1996; Kawahata et al., 1998b). In brief, these parameters were determined with a Yanako CHN Corder MT5 elemental analyzer at AIST. Powdered sample was weighed out about 10 mg and 60 mg on ceramic sample boats for total carbon and total nitrogen concentrations measurement, respectively. For OC contents determination samples were weighed out 95 mg and 1 N HCl was added to remove carbonate within ceramic sample boats. After 12 h the samples were dried up to take off HCl and water at 50°C for at least 3 h until the determination of carbon. Carbonate is calculated as follows:

$$\text{Carbonate} = (\text{Total carbon content} - \text{OC content}) \times 8.333 \quad (1)$$

The relative standard deviations of carbonate, OC, total nitrogen and biogenic opal were 1%, 7%, 8% and 4% in the case of duplicate analyses for their contents of 90 wt%, 0.2 wt%, 0.02 wt% and 10 wt%, respectively.

Biogenic opal contents were determined using a modification of the method developed by Mortlock and Froelich (1989). Samples of 20 mg after removing carbonate by acidification and OM with H_2O_2 were digested in 10 ml of a 7% Na_2CO_3 solution at 85°C for 5 h in 20-ml polyethylene bottles, followed by measurement of Si through molybdate-blue spectrophotometry.

Sediment samples for foraminiferal stable isotopic analysis were disaggregated and wet-sieved with a 63-μm pore size sieve. Forty to fifty specimens of *Globorotalia inflata*, >250 μm in size, were picked for $\delta^{18}O$ estimation using a Finnigan MAT 252 of the Mountain Mass Spectrometry. The oxygen isotopic data are reported in δ notation relative to the Peedee belemnite (PBD) standard. The standard deviation for the $\delta^{18}O$ was ± 0.04‰.

Contents of inorganic elements were measured with inductively coupled plasma atomic emission spectrometry (ICP-AES) and inductively coupled plasma mass spectrometry (ICP-MS) at AIST. Samples were decomposed according to the following procedure: an aliquot of 100 mg of grained powder sample was weighed into a 50-ml Teflon beaker, which was placed on a hot plate. 3 ml of $HClO_4$, 2.5 ml of HCl and HNO_3 and 5 ml of HF were added. After the sample was decomposed once at 95°C for 10 h and twice at 140°C for 12 h, the solutions were diluted with 5 ml of HNO_3 and distilled MilliQ® water to adjust the total volume to 100 ml. Thus prepared sample solution was analyzed by Jobin-Yvon-38 ICP-AES and HP-4500 ICP-MS analyzers. Reference rock standards provided by the Geological Survey of Japan (JB-2, JA-2, JG-1A, JG-2, JR-1) as well as standard solutions prepared from pure elemental standard solutions were used for calibration. The relative standard deviation of >3 ppm for major and minor elements was less than 1% for contents in the sediments while for trace elements it was less than 5%.

Dry bulk density (DBD) was determined directly by sampling a known volume of sediment with paleomagnetic cubes. The dry weight of these samples was determined and divided by the wet volume of the sample to obtain the DBD. Errors associated with the estimation of box weights are in the order of ± 0.04 g. Incomplete filling or compaction may give errors in the order of ± 0.1 g resulting in total error of approximately ± 0.02 g cm^{-3}.

To quantify the true variability of each sedimentary component, eliminating some biased

←

Fig. 2. The values of $\delta^{18}O$, age and time control points in cores NGC108 (solid square and black arrow, respectively) and S2612 (open square and white arrow, respectively) (a). The SPECMAP stack $\delta^{18}O$ record is presented for comparison (solid line). Time series records of LSR (b), lithogenics (c), carbonate (d), biogenic opal (e), OC (f), and $C_{Organic}/N$ atomic ratio (g).

percentage data, we determined the mass accumulation rate (MAR: mg cm^{-2} kyr^{-1}) of each component separately. Conversion of weight percent of the component to the MAR was accomplished using the following equation:

$$MAR = 1000 \times [Comp/100] \times DBD \times LSR \quad (2)$$

where Comp is the content of each component in wt%, DBD is the sediment dry bulk density in g cm^{-3}, and LSR is the linear sedimentation rate in cm kyr^{-1} for each sample.

4. Results

4.1. Biogenic component in core NGC108

The stratigraphic framework is based on oxygen isotope record of planktonic foraminifer *Globorotalia inflata*. The $\delta^{18}O$ stratigraphy is characterized by glacial–interglacial $\delta^{18}O$ amplitudes of approximately 0.6–2.4‰. The stratigraphy is used to establish a simple age model. The definition of oxygen isotope stage (OIS) and conversion into absolute ages follow the time scale of SPECMAP stack (Imbrie et al., 1984) (Fig. 2a). It shows that the record of this core reaches back to OIS 6. The age–depth relationship in the core is presented in Table 1a. The age model of the core yields LSR from 2.25 to 4.70 cm kyr^{-1}, averaging 3.6 cm kyr^{-1} (Fig. 2b).

Carbonate accounts for 27.4–52.3 wt% with a mean value of 39.8 wt% (Fig. 2d). The minima exist in glacial OIS 2 and 4. The carbonate contents in core NGC108 are lower than in core S2612 during the last 180 kyr, but display a similar pattern which has maxima in interglacial times and minima in glacial times. The biogenic opal contents fluctuate from 4.2 to 9.1 wt% with an average value of 6.2 wt%. High values are observed in OIS 6 (Fig. 2e). OC contents in core NGC108 vary between 0.19 and 0.87 wt%, with a mean value of 0.48 wt% (Fig. 2f). The maxima occur in OIS 2, around 48 ka, OIS 4, and late OIS 6. The $C_{Organic}/N$ ratio varies from 2.8 to 8.8, and the mean value is 6.0 (Fig. 2g). High values are found in OIS 2, early OIS 3 to OIS 4, and OIS 6 generally accompanied by higher OC contents.

The $MAR_{Carbonate}$ ranges from 438 to 1467 mg cm^{-2} kyr^{-1}, with a mean value of 827 mg cm^{-2} kyr^{-1}. The lower $MAR_{Carbonate}$ values are found at the core top, in OIS 2/3 and 4/5 boundaries (Fig. 3b). The MAR_{Opal} varies from 58 to 214 mg cm^{-2} kyr^{-1}, with an average value of 137 mg cm^{-2} kyr^{-1}. The higher $MARs_{Opal}$ occur

Table 1a
Age picked and LSR in the studied cores

Depth in core (cm)	Estimated age (kyr)	Isotopic event	Linear sedimentation rate (cm kyr^{-1})
Core NGC108			
0	0		
			2.25
28	12	2.0	
			4.20
199	53	3.3	
			4.33
252	65	4.2	
			2.79
428	128	6.0	
			4.70
536	151	6.4	
			3.19
640	183	6.6	
Core S2612			
0	0		
			1.63
31	19	2.2	
			1.18
71	53	3.3	
			1.33
87	65	4.2	
			0.63
123	122	5.5	
			0.62
131	135	6.2	
			1.56
187	171	6.5	
			1.74
227	194	7.1	
			0.36
243	238	7.5	
			1.05
263	257	8.3	
			1.57
310	287	8.5	

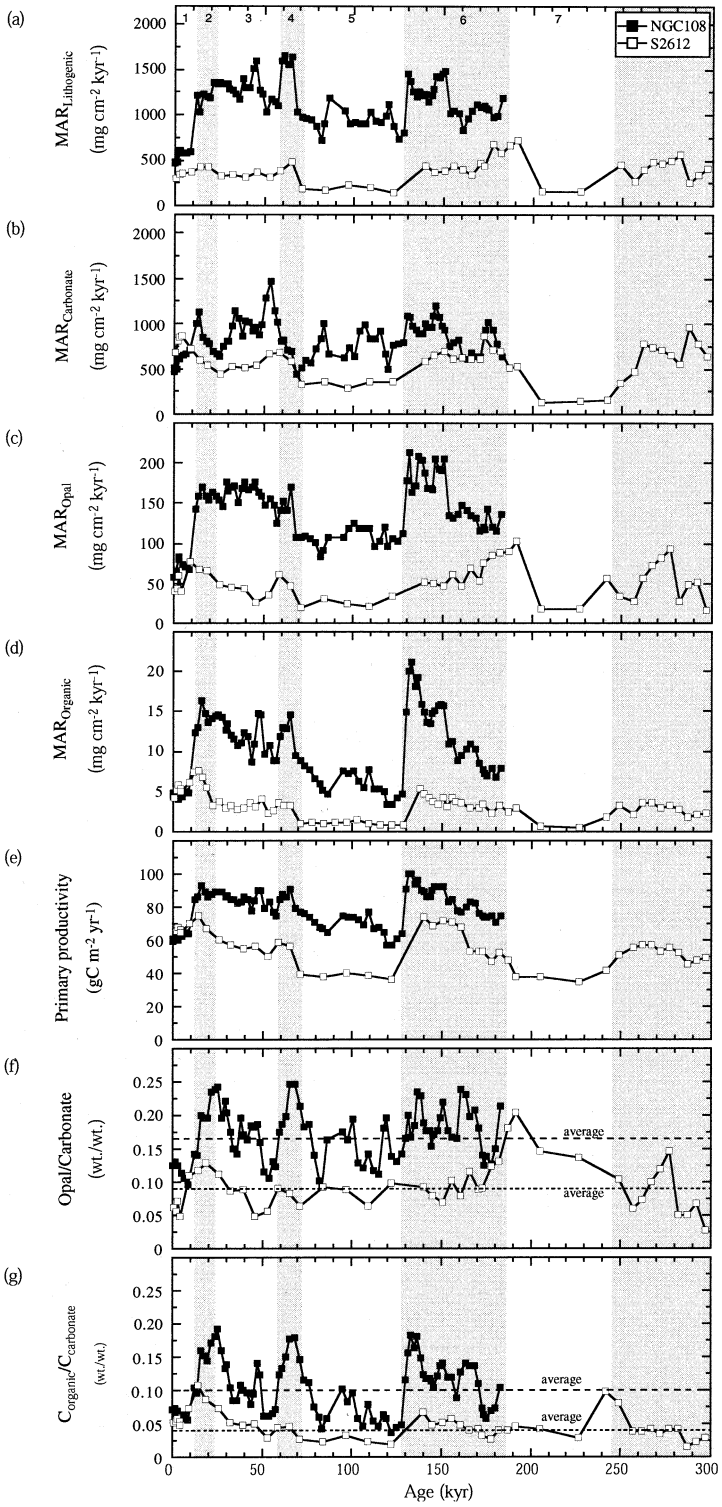

Fig. 3. Time series of $MAR_{Lithogenics}$ (a), $MAR_{Carbonate}$ (b), MAR_{Opal} (c), $MAR_{Organic}$ (d), primary productivity (e), opal/carbonate weight ratios (f), and $C_{Organic}/C_{Carbonate}$ weight ratios (g).

in OIS 2–4 and late OIS 6 (Fig. 3c). The $MAR_{Organic}$ ranges from 3.3 to 21.2 mg cm^{-2} kyr^{-1} (average 10.2 mg cm^{-2} kyr^{-1}). The maxima generally occur in the glacials: OIS 2–4 and late OIS 6 (Fig. 3d). The MAR_{Opal} and $MAR_{Organic}$ give similar profiles. The lithogenics content was calculated as follows:

$$\text{Lithogenics} = \text{Total} - \text{Carbonate} - \text{Opal} - (\text{OC} \times 1.8) \quad (3)$$

Lithogenics constitutes from 42 to 86 wt%, with a mean of 53 wt% (Fig. 2c). The MAR of lithogenics ($MAR_{Lithogenics}$) ranges between 468 and 1645 mg cm^{-2} kyr^{-1}. The mean value is 1098 mg cm^{-2} kyr^{-1}. The maxima of $MAR_{Lithogenics}$ occur around 48 ka, OIS 4, and late OIS 6 (Fig. 3a).

4.2. Sedimentation of inorganic elements in core NGC108

High concentrations of Al_2O_3, TiO_2 and FeO* are observed in OIS 2/3 boundary, OIS 4, early OIS 5 and early OIS 6. CaO and Sr concentrations show peaks in OIS 1, early OIS 3 and late OIS 5. MgO, Zn, Cr and Be concentrations have three large maxima in OIS 2/3 boundary, around 48 ka and OIS 4 with relatively high values in OIS 6. MnO_2 and Ba contents give large peaks at the core top. Similar profiles are observed in Cu and Ni contents with high values at the core top, OIS 2/3 boundary, around 48 ka, OIS 6.

4.3. Biogenic component in core S2612

A detailed 299-kyr-long record of oxygen isotopic values and the MARs of biogenic components have already been reported (Kawahata et al., 1999). Carbonate makes up 16.2–75.6 wt% (average 55.2 wt%) of the sediments (Fig. 2d). The $MAR_{Carbonate}$ ranges from 116 to 940 mg cm^{-2} kyr^{-1} with an average value of 566 mg cm^{-2} kyr^{-1} (Fig. 3b). The MAR_{Opal} ranges between 17 and 103 mg cm^{-2} kyr^{-1}, averaging 51 mg cm^{-2} kyr^{-1} (Fig. 3c). MAR_{Opal} maxima are in OIS 1/2, 3/4, and 6/7 boundaries and middle OIS 8. OC forms 0.14–0.70 wt% of the sediments. The average value is 0.31 wt% (Fig. 2f). The mean $C_{Organic}/N$ atomic ratio is 7.8 (Fig. 2g). The $MAR_{Organic}$ ranges between 0.47 and 7.55 mg cm^{-2} kyr^{-1} (Fig. 3d) with a mean value of 3.16 mg cm^{-2} kyr^{-1}. Relatively high $MAR_{Organic}$ occurs in OIS 2, 6 and 8. Primary productivity records, estimated by using an empirical formula proposed by Sarnthein et al. (1988), have maxima of primary productivity at late OIS 2, late OIS 4, late OIS 6 and OIS 8 (Fig. 3e).

4.4. Sedimentation of inorganic elements in core S2612

High concentrations of Al_2O_3 are observed around OIS 4, 7 and early OIS 8. TiO_2, FeO* and MgO have similar profiles except in OIS 7. CaO and Sr concentrations show a high value in OIS 1, early OIS 3, OIS 6, OIS 8. Higher concentrations of Zn, Cr and Be are found in OIS 7. Large peaks of MnO_2, Ba, and Ni contents occur at the core top. Cu concentration marks three peaks in OIS 3, 4 and 7.

5. Discussion

5.1. OC accumulation and paleoproductivity

OM in sediments is commonly a mixture of marine and terrestrial origins. In general, $C_{Organic}/N$ ratios provide useful information on sources of the OM. Terrestrial and marine OM show $C_{Organic}/N$ ratios of >20 (Hedges and Parker, 1976) and 6–7 (Emerson and Hedges, 1988), respectively. Several samples which have very low OC values of $<0.4\%$ show $C_{Organic}/N$ ratios below 5. It could be attributed to a higher contribution of inorganic nitrogen (fixed as ammonium ions in the interlayers of clay minerals, especially illite) and/or more preservation of organic nitrogen compounds by adsorption to clay minerals protecting them against bacterial attack (Stevenson and Chen, 1972; Müller, 1977). Settling particles obtained by sediment trap deployed at the transition zone showed annual mean $C_{Organic}/N$ atomic ratios of 7.5–8.6 (Kawahata et al., 1998a). More than 40% of total nitrogen of

these settling particles originated from peptide amino acids which were synthesized by marine organisms (Gupta, personal communication). In addition, Naraoka and Ishiwatari (2000) demonstrated that terrestrial OM is quite limited for OM in the surface sediments in the western Pacific (38°N, 142–147°E) based upon the analysis of $\delta^{13}C$ of bulk OC, fatty acid, and alkanes. Therefore, OC in cores NGC108 and S2612 can be mainly of marine origin.

Since $MARs_{Organic}$ generally reflect primary productivity in the surface water rather than the influence of decomposition by dissolved oxygen in the bottom water if OC is of marine origin (Jahnke, 1990; Kawahata et al., 1998b), higher $MAR_{Organic}$ in core NGC108 than in core S2612 probably indicates higher primary productivity at the former site. Rühlemann et al. (1999) discussed factors controlling OC preservation in marine sediments and offer some difference on paleoproductivity estimates using different equations. Therefore the calculated productivity could be rough estimates. We calculated the paleoproductivity by using the equations proposed by Müller and Suess (1979), Stein (1986) and Sarnthein et al. (1988, 1992), and compared the results on the top sediments. Compared with modern values around 60 g C m^{-2} yr^{-1} in this region (Berger, 1989), the values using the formula of Müller and Suess (1979) were too low while those using the formula of Sarnthein et al. (1992) were too high. The best fit values (61 g C m^{-2} yr^{-1} in core NGC108 and 65 g C m^{-2} yr^{-1} in core S2612) were deduced from the formula of Sarnthein et al. (1988). It was an empirical equation to estimate paleoproductivity based on the relationships among OC accumulation rates in surface sediments, sedimentation rates, water depths, and measured (recent) surface water productivity.

$$PP^2 = 0.0238 \times \%OC^{0.6429} \times LSR^{0.875} \times DBD^{0.5364} \times Z^{0.8292} \times (LSR(1-\%C/100))^{-0.2392} \quad (4)$$

where PP is primary productivity (g C m^{-2} yr^{-1}), %OC is OC content (wt%), LSR is linear sedimentation rate (cm kyr^{-1}), DBD is dry bulk density (g cm^{-3}), and Z is water depth (m).

The calculated PP record in core NGC108 for the last 180 kyr varies from 57 to 100 g C m^{-2} yr^{-1} with a mean value of 79 g C m^{-2} yr^{-1} (Fig. 3e). The higher PP values occur in OIS 2–4 and late OIS 6. The minima are observed in OIS 1 and early OIS 5. On the other hand, the PP estimates of S2612 (Kawahata et al., 1999) display a similar

Table 2
Correlation factors between each component content in core NGC108

	OC	Carbonate	Biogenic opal	Al_2O_3	TiO_2	FeO*	CaO	MgO	MnO_2	Sr	Zn	Cr	Be	Ba	Cu
Carbonate	−0.45														
Biogenic opal	0.71	−0.42													
Al_2O_3	0.15	−0.89	0.08												
TiO_2	0.14	−0.84	0.05	0.97											
FeO*	0.23	−0.73	0.14	0.73	0.77										
CaO	−0.44	0.99	−0.40	−0.90	−0.85	−0.74									
MgO	0.60	−0.79	0.41	0.74	0.76	0.82	−0.81								
MnO_2	−0.22	0.33	−0.18	−0.34	−0.32	−0.27	0.37	−0.37							
Sr	−0.53	0.95	−0.47	−0.81	−0.78	−0.70	0.96	−0.82	0.47						
Zn	0.47	−0.77	0.27	0.77	0.75	0.68	−0.79	0.84	−0.29	−0.78					
Cr	0.69	−0.67	0.50	0.61	0.62	0.61	−0.69	0.92	−0.39	−0.72	0.76				
Be	0.57	−0.71	0.44	0.69	0.67	0.63	−0.73	0.89	−0.29	−0.72	0.82	0.92			
Ba	−0.44	0.54	−0.33	−0.49	−0.50	−0.46	0.58	−0.60	0.75	0.68	−0.44	−0.63	−0.49		
Cu	0.14	−0.20	−0.11	0.28	0.32	0.20	−0.17	0.27	0.37	−0.06	0.31	0.23	0.27	0.24	
Ni	0.31	−0.30	0.13	0.27	0.29	0.42	−0.32	0.48	0.45	−0.29	0.58	0.41	0.50	0.09	0.45

FeO*: calibrated as total iron.
Original data tables are electronically archived in Marine Geology and other web sites (**background data set**[2]).

Table 3
Correlation factors between each component content in core S2612

	OC	Carbonate	Biogenic opal	Al_2O_3	TiO_2	FeO*	CaO	MgO	MnO_2	Sr	Zn	Cr	Be	Ba	Cu
Carbonate	0.17														
Biogenic opal	0.02	−0.39													
Al_2O_3	−0.28	−0.97	0.39												
TiO_2	−0.23	−0.74	0.33	0.81											
FeO*	−0.04	−0.58	0.20	0.65	0.90										
CaO	0.13	0.97	−0.39	−0.95	−0.68	−0.53									
MgO	0.06	−0.47	0.24	0.56	0.88	0.93	−0.39								
MnO_2	0.36	0.36	−0.25	−0.46	−0.49	−0.46	0.33	−0.46							
Sr	0.13	0.97	−0.39	−0.96	−0.71	−0.57	0.95	−0.48	0.46						
Zn	0.28	−0.67	0.35	0.73	0.84	0.77	−0.68	0.80	−0.22	−0.68					
Cr	0.04	−0.47	0.36	0.56	0.83	0.75	−0.39	0.91	−0.50	−0.47	0.82				
Be	−0.21	−0.88	0.48	0.93	0.80	0.60	−0.85	0.61	−0.49	−0.88	0.78	0.71			
Ba	0.08	0.20	−0.16	−0.20	−0.18	−0.23	0.07	−0.32	0.57	0.25	−0.04	−0.31	−0.24		
Cu	0.15	0.04	−0.11	0.02	0.18	0.18	0.04	0.23	0.11	0.05	0.27	0.20	0.07	0.21	
Ni	0.60	0.29	−0.15	−0.38	−0.24	−0.16	0.29	−0.05	0.84	0.38	0.13	−0.07	−0.31	0.37	0.24

FeO*: calibrated as total iron.
Original data tables are electronically archived in Marine Geology and other web sites (**background data set**[2]).

profile with maxima in glacial times. However, the values range between 66 and 75 g C m^{-2} yr^{-1}, and are always lower than those in core NGC108.

OC is highly correlated with biogenic opal content in core NGC108 ($r = 0.70$) in contrast to a poor correlation in core S2612 ($r = 0.03$) (Tables 2 and 3), which suggests that biogenic opal could play a significant role in primary productivity at site NGC108. Since NGC108 (36°N) and S2612 (32°N) are located in the northern part and near the southern edge of the transition zone, respectively, both sites should be sensitively influenced by the Subarctic front migration. In fact, sediment trap experiments reported that OC and biogenic opal fluxes increased markedly from the transition to Subarctic zones along 175°E (Kawahata et al., 1998a). The fluxes were 4.8, 5.2, 11.6 and 14.6 mg m^{-2} day^{-1} for OC and 3.2, 3.7, 17.5 and 143.4 mg m^{-2} day^{-1} for biogenic opal at sites 6 (30°00.1′N), 5 (34°25.3′N), 7 (37°24.2′N) and 8 (46°07.2′N), respectively. On the other hand, carbonate fluxes were 30.2, 23.3, 41.5 and 38.5 mg m^{-2} day^{-1} at sites 6, 5, 7 and 8, respectively, which fluctuated much less than biogenic opal flux.

As the sediment trap experiments show a large increase in annual biogenic opal/carbonate ratios from the transition zone to the Subarctic zone, the ratios in the cores could provide information about the latitudinal shift of the Subarctic front with time if the carbonate dissolution effect is not significant. The lysocline depth at the Shatsky Rise is approximately 3200 m at present (Chen et al., 1988), which is comparable to the seafloor depth (3390 m) at site NGC108. Pacific deep water is less corrosive during glacial times while more during interglacial times, when the carbonate content was, actually, significantly reduced in the equatorial Pacific (Farrell and Prell, 1989; Kahawahata, 1999). However, no definite fluctuation on carbonate content was observed through glacial and interglacial times in core NGC108. Therefore it is suggested that the dissolution effect has not been a primary factor to control carbonate content in the core.

Fig. 3f shows that core NGC108 has higher values of opal/carbonate ratios (0.09–0.25) than S2612 (0.05–0.13) through time, even during interglacial times. It suggests that the surface water around site NGC108 has been affected more by Subarctic water mass in contrast to site S2612 which is more affected by Central water mass. These ratios in core NGC108 are generally higher in OIS 2/3 boundary, OIS 4 and OIS 6, which

correspond roughly to periods when $MAR_{Organic}$ and PP are also elevated. It is consistent with the southward shift of the Subarctic front in OIS 2, 4, and 6 based upon the planktonic foraminifer assemblage proposed by Thompson and Shackleton (1980). They suggested that the Subarctic front might have reached as far south as 35–38°N and 32–35°N in OIS 2 and 6, respectively. The Subarctic front in the western North Pacific identified by the 5°C isotherm is seen at around 41°N at present (Tomczak and Godfrey, 1994). However, the opal/carbonate ratio in core S2612 remains fairly constant during the last 180 kyr relative to that in core NGC108. This may suggest that the southern transition zone is more stable than the northern transition zone. Therefore the transition zone between Subarctic and Central water masses might be smaller in latitudinal width in the OIS 2/3 boundary, OIS 4 and OIS 6 relative to that during interglacial times. It is consistent with pollen and spore results. It demonstrated that the warm-temperate–subtropical forest pollen, originating mainly from around the South China Sea, contributed much to the sediments on the Hess Rise at the mid-latitude of the North Pacific during the glacial times, which means that the Kuroshio Extension fluctuated latitudinally only to a small extent (Kawahata and Ohshima, 2002).

The sedimentary cycle of OC and carbonate carbon production and preservation exerts a large influence on the amount of CO_2 in the oceans and atmosphere. Every mole of $CaCO_3$ formed in the sea by the combination of Ca^{2+} and HCO^{3-} liberates a mole of CO_2. Conversely the burial of OC in sediments can be thought of as CO_2 removal from the ocean–atmosphere system (e.g., Farrell and Prell, 1989; Shaffer, 1993). In this sense, the $C_{Organic}/C_{Carbonate}$ rain ratio preserved in sediments is a proxy indicator of the long-term CO_2 budget, that is, the lower the $C_{Organic}/C_{Carbonate}$ rain ratio, the more CO_2 is available to the environment from the relative preservation of these components. The $C_{Organic}/C_{Carbonate}$ rain ratio was apparently higher in core NGC108 than in core S2612 during the last 180 kyr (Fig. 3g). Especially an increase in the rain ratio in OIS 2, middle OIS 3, OIS 4 and OIS 6 promotes the carbon removal from surface water to deep sea.

5.2. Sedimentation of inorganic elements

Based upon correlation between each element, 13 elements were classified into four groups: (1) terrigenous components (Al_2O_3, TiO_2, FeO*), (2) biogenic calcareous material (CaO, Sr), (3) biogenic-scavenged elements (MgO, Zn, Cr, Be) and (4) the other elements (MnO_2, Ba, Cu, Ni).

5.2.1. Terrigenous components

It has been concluded that the alumino-silicate minerals such as feldspar and clay minerals could be mainly transported from the Asian continent to the Hess Rise through the atmosphere (Fig. 1) based upon a highly positive correlation of the aerosol quartz chemically isolated from sediments with Al_2O_3 content and MAR (correlation coefficients of 0.88 and 0.91, respectively) (Kawahata et al., 2000). It is consistent with the fact that volcanic ash quartz accounts for approximately 25% of total quartz in the S2612 sediments based upon particle size and shape analysis of quartz (Okamoto et al., 2002). Therefore a quarter of alumino-silicate originates from volcanics while the rest is of aerosol origin. TiO_2 and FeO* were highly correlated with Al_2O_3 (Tables 2 and 3). Ti/Al and Fe/Al (w/w) ratios (Table 4) were comparable to those of Nanjing loess (0.051 and 0.28, respectively) (Taylor et al., 1983). These results indicate

Table 4
Comparison of metal/Al ratios

Metal/Al ratio	NGC108 (w/w)	S2612 (w/w)	Nanjing Loess (w/w)
Ti/Al	0.047	0.047	0.051
Fe/Al	0.540	0.530	0.280
Ca/Al	4.690	8.658	0.062
Mg/Al	0.287	0.282	0.103
Mn/Al	0.018	0.022	0.008
$Sr/Al \times 10^{-4}$	238	426	6.75
$Cr/Al \times 10^{-4}$	7.85	7.05	4.48
$Zn/Al \times 10^{-4}$	18	15	5.06
$Be/Al \times 10^{-4}$	0.26	0.26	0.16
$Ba/Al \times 10^{-4}$	297	369	31

Nanjing loess data from Taylor et al. (1983).
Original data tables will be electronically archived in Marine Geology or other web sites (**background data set**[2]).

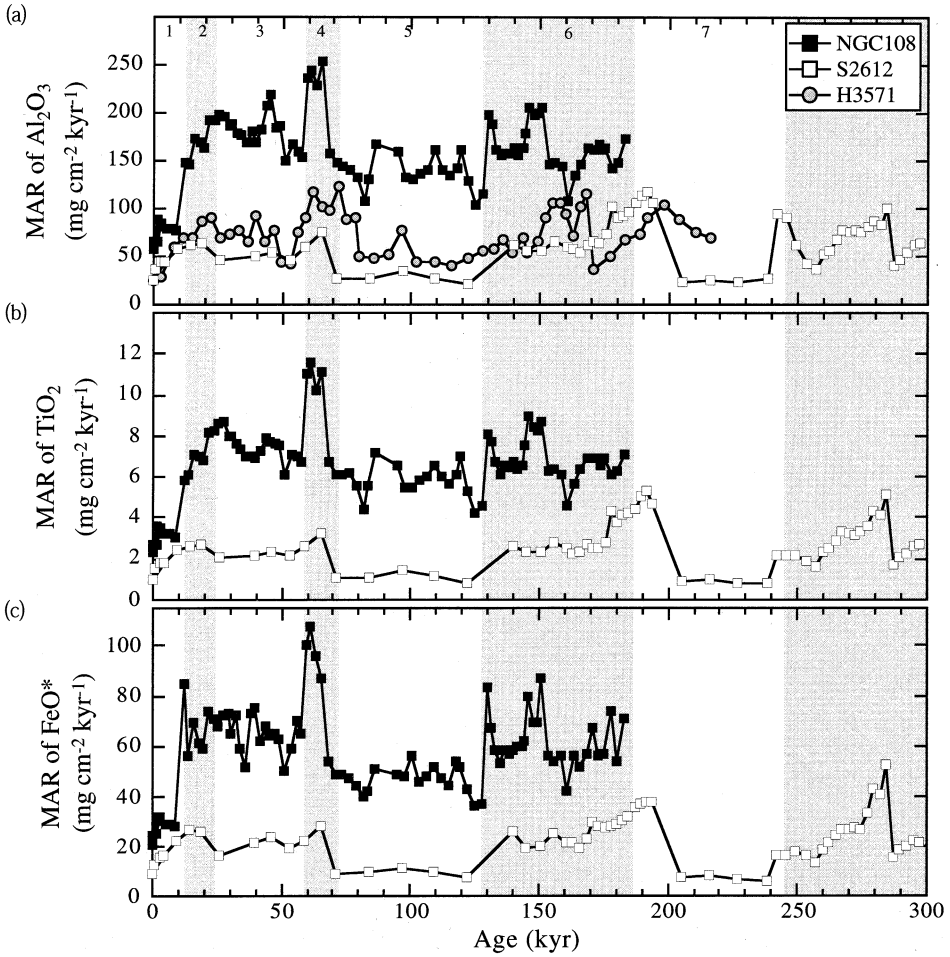

Fig. 4. Time series profiles of MARs of Al_2O_3 (a), TiO_2 (b), FeO* (c). The shaded circles in panel (a) display the result from H3571 published by Kawahata et al. (2000).

that these three elements belong to terrigenous components. The MARs of Al_2O_3, TiO_2 and FeO* were elevated in OIS 2, 3 and 4 and late OIS 6 in core NGC108 while they were higher in early OIS 1, OIS 2, 4 and 6 in core S2612 (Fig. 4). These profiles are roughly consistent with that of MAR of Al_2O_3 observed on the Hess Rise (Kawahata et al., 2000).

5.2.2. Biogenic calcareous elements

Chinese loess is depleted in Sr while biogenic calcareous skeletons are enriched in Sr (Table 4). Sr is highly correlated with CaO ($r = 0.96$ in NGC108; $r = 0.95$ in S2612), indicating that Sr replaces some Ca in the biogenic calcite or aragonite crystals. Sr/Ca weight ratios of 50.8×10^{-4} and 35.2×10^{-4} in cores NGC108 and S2612 were comparable to that observed in common biogenic carbonate (52.5×10^{-4}) (Turekian, 1964).

5.2.3. Biogenic-scavenged elements

Although MgO, Zn, Cr, and Be are correlated with Al_2O_3 (Tables 2 and 3), Mg/Al, Zn/Al, Cr/Al and Be/Al (w/w) ratios were about 1.6–2.9 times higher than that of mean relative Nanjing loess abundance (Table 4). In addition, these elements were fairly correlated with both OC ($r = 0.60$,

0.47, 0.69 and 0.57, respectively) and biogenic opal ($r = 0.41$, 0.27, 0.50 and 0.44, respectively) in core NGC108, which is enriched in biogenic opal. In contrast, these elements showed no correlation in core S2612. Kawahata et al. (2000) reported that the aerosol silica supply to the ocean may have some potential to affect the burial of biogenic silica into sediments. Particle sizes of these dust minerals and volcanic ash on the Hess Rise are commonly less than 8 μm and around 10 μm, respectively. Such small size of particles is difficult to remove rapidly from the surface ocean. As indicated by Honjo et al. (1982), biogenic aggregates such as diatoms and coccolithophores cause accelerated sinking of small non-biogenic particles due to scavenging and agglutination. Incorporated or attached non-biogenic particles may accelerate the sinking rates of pellets or amorphous aggregates and reduce the particle residence time and degradation rate (Haake and Ittenot, 1990). Diatoms, coccolithophores and foraminifers were major biogenic debris in settling particles (Tanaka and Eguchi, personal communication). Therefore sedimentation of these four elements could be affected by terrestrial input and biological vertical transport process.

5.2.4. The other elements

Sediment trap experiments reported that the Mn concentration and the Mn/Al (w/w) ratio increase continuously with water depth (Brewer et al., 1980; Tsunogai et al., 1982; Martin et al., 1985; Masuzawa et al., 1989). Therefore Mn is classified into the scavenging type of elements; it is, however, also a very sensitive element for oxidation/redox condition. When Mn can be dissolved under reduced condition such as in organic-rich layers of sediments, it accumulates under oxidized condition such as in the surface oxidized layer. Sometimes such deposited Mn is dissolved again when being reduced and redistributed in the sedimentary column (Lynn and Bonatti, 1965; Bonatti et al., 1971; Burdige and Gieskes, 1983). These processes may be responsible for enrichment of MnO_2 in the surface 20-cm-thick sediments of core NGC108, where Ba also showed high values (Fig. 5). The subsurface maxima in

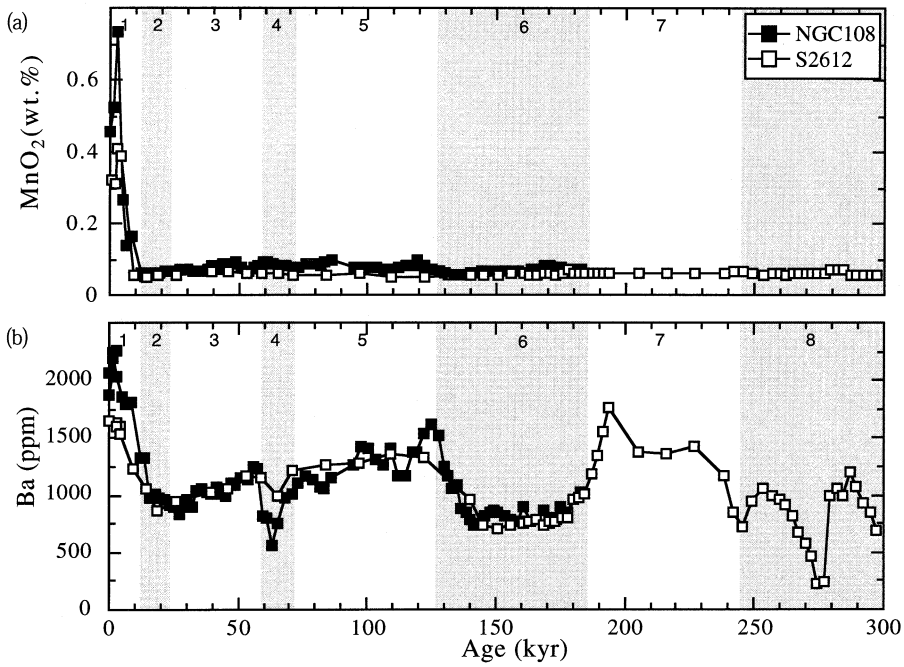

Fig. 5. Time series profiles of contents of MnO_2 (a) and Ba (b).

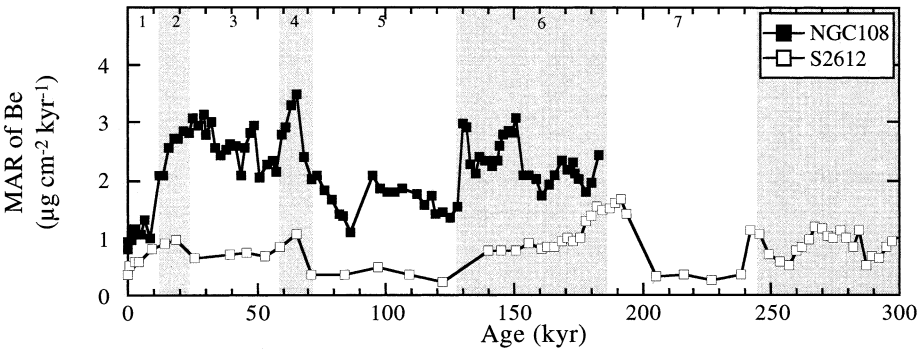

Fig. 6. Time series profiles of MAR of Be.

Mn and Ba may be attributed to the observation that dissolved Mn and Ba diffuse downwards into the sediment under anoxic condition and upwards into the overlying oxic horizon where they are reprecipitated as Mn oxides and barite, respectively.

Ba contents show some fluctuation with glacial/interglacial variations. In cores NGC108 and S2612 high values are observed in OIS 1, 5, and 7 while low values are seen in OIS 2, 3, 4, 6 and 8. Although Ba has been proposed as a paleoproductivity indicator, Ba is not correlated with OC. Instead, Ba contents are correlated with carbonate contents in core NGC108 ($r = 0.58$), which suggests that carbonate may be a major carrier for Ba. This observation is consistent with a low terrigenous contribution. Assuming that the mean Ba/Al (w/w) ratio of the continental crust is 68.3×10^{-4} (Taylor and McLennan, 1985) and the mean Al contents in cores NGC108 and S2612 are 3.96 wt% and 3.14 wt%, respectively, this could result in a relative contribution of Ba of 100–150 ppm.

5.3. Fluctuation in Be precipitation

Of MgO, Zn, Cr and Be, Be has been extensively studied with respect to its behavior in the ocean because of its potential in dating marine deposits (e.g., Bourlés et al., 1989; Sharma et al., 1989). It has been generally envisioned that in the ocean, ^{10}Be (half-life 1.5 Ma) is chiefly supplied from the atmosphere by spallation of oxygen and nitrogen atoms by galactic cosmic rays (Lal and Peters, 1967) whereas the stable counterpart ^{9}Be, as a weathering product of continental rocks, enters the ocean via riverine and eolian transports. Although the absolute concentration of ^{10}Be is subject to variation, due to changes in sedimentary composition and accumulation rates and to variations in the efficiency of its scavenging from the water column, ^{9}Be is a major isotope for Be abundance because the ^{10}Be/^{9}Be ratio is 0.8–3.2×10^{-7} in the Pacific seawater (Kusakabe et al., 1990). Simple mass balance calculations have suggested that alumino-silicate aerosols may be a significant source of ^{9}Be to the oceans (Kusakabe et al., 1991; Ku et al., 1990; Brown et al., 1992), but it has also been proposed that they provide active surfaces for scavenging removal of ^{10}Be (Sharma et al., 1987; Southon et al., 1987). The nutrient-like recycling behavior for both Be isotopes, involving surface scavenging and deep water regeneration, is manifested by the vertical profiles in the Pacific. In contrast, in the equatorial Atlantic, the surface enrichment of ^{9}Be can be ascribed to the eolian dust input mainly from the Sahara Desert (Prospero et al., 1981). The excess inputs of ^{9}Be overtake the surface particulate scavenging mechanism, and prevent the establishment of a surface deficiency of ^{9}Be. The MAR of Be in OIS 2, 3 and 4 and middle OIS 6 at site NGC108 was about four times higher than that observed at site S2612 (Fig. 6). These time series profiles were generally consistent with that of aerosol particles. MAR of mineral aerosol ($MAR_{Aerosol}$) maxima occur in OIS 4 to latest OIS 5, middle OIS 6, and moderate maxima occur

in early OIS 1 to 2, late OIS 3 and middle OIS 3 on the Hess Rise (Kawahata et al., 2000). The $MAR_{Aerosol}$ varies from 156 to 732 mg cm^{-2} kyr^{-1} on the Hess Rise, which is consist with $MAR_{Lithogenics}$ obtained between cores NGC108 and S2612.

Scavenging is a general term that includes adsorption, absorption, complexation and biological uptake (Anderson et al., 1994). While the composition of particulate matter certainly influences the partitioning of reactive chemical substances between dissolved and particulate phases, the flux of particulate matter through the water column seems to be the principal factor regulating the overall intensity of scavenging (Lao et al., 1992, 1993). Sharma et al. (1987) indicated that primary carrier phases for the Be isotopes in the water column might be alumino-silicates based upon good correlation among ^{10}Be, ^{9}Be and ^{27}Al. It is also suggested that scavenging of Be may be related to opal productivity in surface waters (Lao et al., 1992). In contrast, biogenic carbonates may not contribute significantly to nuclide scavenging (Southon et al., 1987). Actually Be is correlated not with carbonate but with OC, biogenic opal and lithogenics in core NGC108. On the other hand, Be has only a positive relation with biogenic opal and lithogenics in the carbonate-rich core S2612. These observations suggest that alumino-silicate has enhanced aerosol Be inputs during glacial times, when higher fluxes of alumino-silicate, OC and biogenic opal could work as a scavenging carriers.

Be is one of the most particle-reactive chemical substances in the ocean, resulting in the most enhanced deposition (Anderson et al., 1994). These results provide important implications for the past geochemical cycle of Be. The residence time of Be in the oceans is relatively short, on the order of the oceanic mixing time (Anderson et al., 1990; Kusakabe et al., 1991). Therefore enhanced eolian input and elevated primary productivity in association with biogenic opal during glacial times have modified Be abundance in the oceanic reservoir rapidly. This means that, regarding Be, the ocean reservoir is not in a steady-state condition but fluctuates largely in response to climatic change.

6. Summary and conclusion

Detailed records of contents and MARs of biogenic components and inorganic elements were presented from the Shatsky Rise in the western North Pacific during the late Quaternary in order to verify the fluctuation of biogenic sedimentation and the related vertical transport of inorganic elements.

(1) OM around the Shatsky Rise is mainly of marine origin based upon the mean $C_{Organic}/N$ atomic ratios of 6.0 and 7.8 from cores NGC108 and S2612, respectively. The high correlation between OC and biogenic opal contents observed in core NGC108 is in contrast to the poor correlation in core S2612. Although the PP estimated in cores NGC108 and S2612 generally increases during glacial times and decreases during interglacial times, the PP, biogenic opal/carbonate ratios and the $C_{Organic}/C_{Carbonate}$ ratios have always been higher in core NGC108 than in core S2612 during the last 180 kyr. These results suggest that the surface water at site NGC108 has been influenced more by Subarctic water in contrast to site S2612, which has been more affected by Central water through time.

(2) The opal/carbonate ratio in core S2612 remains fairly constant relative to that in core NGC108, which may suggest that the transition zone between Subarctic and Central water was narrower in latitude in OIS 2/3 boundary, OIS 4 and OIS 6.

(3) The $C_{Organic}/C_{Carbonate}$ ratio in core NGC108 shows higher values in OIS 2, middle OIS 3, OIS 4 and OIS 6, which indicates that the carbon removal from surface water to deep sea was promoted in these periods.

(4) Thirteen elements are divided into four groups based on correlation between each element in content: (1) terrigenous components (Al, Ti, Fe), (2) biogenic calcareous material (Ca, Sr), (3) biogenic-scavenged elements (Mg, Zn, Cr, Be), and (4) the other elements (Mn, Ba, Cu, Ni). The terrigenous MARs are elevated in OIS 2, 3 and 4 and late OIS 6 in core NGC108 while they are higher in early OIS 1, OIS 2, 4 and 6 in core S2612. Although biogenic-scavenged elements are correlated with Al_2O_3, the ratio of

each element to Al_2O_3 is about 1.6–2.9 times higher than in Nanjing loess. MnO_2 and Ba might be redistributed during the sub-surface reduced condition. Therefore these elements do not record the past environment.

(5) Sedimentation of particle-reactive Be could be accelerated by both enhanced terrigenous input and biogenic vertical transport. Since its residence time in the oceans is relatively short, on the order of the oceanic mixing time, the ocean reservoir regarding Be is not in a steady-state condition but has fluctuated largely in response to climatic change.

Acknowledgements

The authors express their appreciation to Dr. L.P. Gupta for valuable comments which helped improve the manuscript. They thank Prof. R. Stein and an anonymous reviewer for comments to improve the manuscript. This study was supported by the following research programs: 'GCMAPS program (Global carbon cycle and related mapping based on satellite imagery' promoted by the Ministry of Education, Culture, Sports, Science and Technology, 'Study on Paleoceanography' funded by AIST and 'NOPACCS study' consigned to KANSO Ltd. by the New Energy and Industrial Technology Development Organization.

References

Anderson, R.F., Lao, Y., Broecker, W.S., Trumbore, S.E., Hofmann, H.J., Wolfli, W., 1990. Boundary scavenging in the Pacific Ocean: A comparison of ^{10}Be and ^{231}Pa. Earth Planet. Sci. Lett. 90, 287–304.

Anderson, R.F., Fleisher, M.Q., Biscaye, P.E., Kumar, N., Dittrich, B., Kubik, P., Suter, M., 1994. Anomalous boundary scavenging in the Middle Atlantic Bight: evidence from ^{230}Th, ^{231}Pa, ^{10}Be and ^{210}Pb. Deep Sea Res. II 41, 537–561.

Berger, W.H., Adelseck, C.G., Mayer, L.A., 1976. Distribution of carbonate in surface sediments of the Pacific Ocean. J. Geophys. Res. 81, 2617–2627.

Berger, W.H., 1989. Global maps of ocean productivity. In: Berger, W.H., Smetacek, V.S., Wefer, G. (Eds.), Productivity of the Oceans: Past and Present. Wiley, New York, pp. 429–455.

Bonatti, E., Fisher, D.E., Joensuu, O., Rydell, H.S., 1971. Postdepositional mobility of some transition elements, phosphorus, uranium and thorium in deep sea sediments. Geochim. Cosmochim. Acta 35, 189–201.

Bourlés, D., Raisbeck, G.M., Yiou, F., 1989. ^{10}Be and ^{9}Be in marine sediments and their potential for dating. Geochim. Cosmochim. Acta 53, 443–452.

Brewer, P.G., Nozaki, Y., Spencer, D.W., Fleer, A.P., 1980. Sediment trap experiments in the deep North Atlantic: isotopic and elemental fluxes. J. Mar. Res. 38, 703–728.

Brown, E.T., Measures, C.I., Edmond, J.M., Bourlés, D.L., Raisbeck, G.M., Yiou, F., 1992. Continental inputs of beryllium to the oceans. Earth Planet. Sci. Lett. 114, 101–111.

Burdige, D.J., Gieskes, J.M., 1983. A pore water/solid phase diagenetic model for manganese in marine sediments. Am. J. Sci. 283, 29–47.

Chen, C.T.A., Feely, R.A., Gendron, J.F., 1988. Lysocline, calcium carbonate compensation depth, and calcareous sediments in the North Pacific Ocean. Pac. Sci. 42, 237–252.

Dersch, M., Stein, R., 1994. Late Cenozoic records of eolian quartz flux in the Sea of Japan (ODP Leg 128, Sites 798 and 799) and paleoclimate in Asia. Palaeogeogr. Palaeoclimatol. Palaeoecol. 108, 523–535.

Emerson, S., Hedges, J.I., 1988. Processes controlling the organic carbon content of open ocean sediments. Paleoceanography 3, 621–634.

Farrell, J.W., Prell, W.L., 1989. Climatic change and $CaCO_3$ preservation: an 800,000 year bathymetric reconstruction from the central equatorial Pacific ocean. Paleoceanography 4, 447–766.

Haake, B., Ittenot, V., 1990. Die wind-getriebence 'biologiche Pumpe' und der Kohlenstoffentzug im Ozean. Naturwissenschaften 40, 75–79.

Haug, G.H., Maslin, M.A., Sarnthein, M., Stax, R., Tiedemann, R., 1995. Evolution of Pacific sedimentation patterns since 6 Ma (Site 882). In: Rea, D.K. et al. (Eds.), Proc. ODP Sci. Results, 293–301.

Hedges, J.I., Parker, P.L., 1976. Land-derived organic matter in surface sediments from Gulf of Mexico. Geochim. Cosmochim. Acta 40, 1019–1029.

Hesse, P., 1994. The record of continental dust from Australia in Tasman Sea sediments. Quat. Sci. Rev. 13, 257–272.

Honjo, S., Manganini, S.J., Cole, J.J., 1982. Sedimentation of biogenic matter in the deep ocean. Deep Sea Res. 29, 609–625.

Hovan, S.A., Rea, D.K., Pisias, N.G., Shackleton, N.J., 1989. A direct link between the China loess and marine δ^{18}O records: aeolian flux to the Pacific. Nature 340, 296–298.

Hovan, S.A., Rea, D.K., Pisias, N.G., 1991. Late Pleistocene continental climate and oceanic variability recorded in northwest Pacific sediments. Paleoceanography 6, 349–355.

Imbrie, J., Shackleton, N.J., Pisias, N.G., Morley, J.J., Prell, W.L., Martinson, D.G., Hays, J.D., McIntyre, A., Mix, A.C., 1984. The orbital theory of Pleistocene climate: support from a revised chronology of the marine O-18 record. In: Berger, A. et al. (Eds.), Milankovich and Climate, Part 1. Reidel, Dordrecht, pp. 269–305.

Ioka, N., Hatakeyama, Y., Ikehara, K., Tanaka, Y., Nakashima, K., Suzuki, A., 1997. Marine sediments taken during the NH95-1 cruise. In: Nishumura, A. (Ed.), Preliminary Report of NH95-1. Geological Survey of Japan, Tsukuba, pp. 63–80 (in Japanese).

Jahnke, R.A., 1990. Ocean flux studies: A status report. Rev. Geophys. 28, 381–398.

Janecek, T., Rea, D.K., 1985. Quaternary fluctuations in the Northern Hemisphere Trade Winds and Westerlies. Quat. Res. 24, 150–163.

Johnson, L.R., 1979. Mineralogical dispersal patterns of North Atlantic deep-sea sediments with particular reference to eolian dusts. Mar. Geol. 29, 334–345.

Joyce, T.M., 1987. Hydrographic sections across the Kuroshio Extension at 165°E and 175°W. Deep Sea Res. 34, 1331–1352.

Kawahata, H., Eguchi, N., 1996. Biogenic sediments in the Eauripik Rise of the equatorial western Pacific during the last 265 kyr. Geochem. J. 30, 201–215.

Kawahata, H., Suzuki, A., Ohta, H., 1998a. Sinking particles between the Equatorial and Subarctic regions (0°N–46°N) in the Central Pacific. Geochem. J. 32, 125–133.

Kawahata, H., Suzuki, A., Ahagon, N., 1998b. Biogenic sediments in the West Caroline Basin, the western equatorial Pacific during the last 330 kyr. Mar. Geol. 149, 155–176.

Kawahata, H., Ohkushi, K., Hatakeyama, Y., 1999. Comparative Late Pleistocene paleoceanographic changes in the mid latitude boreal and austral western Pacific. J. Oceanogr. 55, 747–761.

Kahawahata, H., 1999. Fluctuations in the ocean environment within the western Pacific warm pool during late Pleistocene. Paleoceanography 14, 639–652.

Kawahata, H., Okamoto, T., Matsumoto, E., Ujiie, H., 2000. Fluctuations of eolian flux and ocean productivity in the mid-latitude north Pacific during the last 200 kyr. Quat. Sci. Rev. 19, 1279–1291.

Kawahata, H., Ohshima, H., 2002. Small latitudinal shift in the Kuroshio Extension during the glacial times evidenced by pollen transportation. Quat. Sci. Rev. 21, 1705–1717.

Ku, T.L., Kusakabe, M., Measures, C.I., Southon, J.R., Cusimano, G., Vogel, J.S., Nelson, D.E., Nakaya, S., 1990. Beryllium isotope distribution in the western North Atlantic: A comparison to the Pacific. Deep Sea Res. 37, 795–808.

Kusakabe, M., Ku, T.L., Southon, J.R., Measures, C.I., 1990. Beryllium isotope in the ocean. Geochem. J. 24, 263–272.

Kusakabe, M., Ku, T.L., Southon, J.R., Liu, S., Vogel, J.S., Nelson, D.E., Nakaya, S., Cusimano, G.L., 1991. Be isotopes in rivers/estuaries and their oceanic budgets. Earth Planet. Sci. Lett. 102, 265–276.

Lao, Y., Anderson, R.F., Broecker, W.S., Trumbore, S.E., Hofmann, H.J., Wolfli, W., 1992. Transport and burial rates of ^{10}Be and ^{231}Pa in the Pacific Ocean during the Holocene period. Earth Planet. Sci. Lett. 113, 173–189.

Lao, Y., Anderson, R.F., Broecker, W.S., Hofmann, H.J., Wolfli, W., 1993. Particulate fluxes of ^{230}Th, ^{231}Pa, and ^{10}Be in the northeastern Pacific Ocean. Geochim. Cosmochim. Acta 57, 205–217.

Lal, D., Peters., B., 1967. Cosmic ray produced radioactivity on the earth. In: Encyclopedia of Physics 46/2. Springer-Verlag, Berlin, pp. 551–612.

Levitus, S., Conkright, M.E., Reid, J.L., Najjar, R.G., Mantyla, A., 1993. Distribution of nitrate, phosphate and silicate in the world oceans. Prog. Oceanogr. 31, 245–273.

LEVITUS94. World Ocean Atlas, 1994, http://ingrid.ldgo.columbia.edu/SOURCES/.LEVITUS94.

Lynn, D.C., Bonatti, E., 1965. Mobility of manganese in diagenesis of deep-sea sediments. Mar. Geol. 3, 457–474.

Martin, J.H., Knauer, G.A., Broenkow, W.W., 1985. VERTEX: the lateral transport of manganese in the northeast Pacific. Deep Sea Res. 32, 1405–1427.

Masuzawa, T., Noriki, A., Kurosaki, T., Tsunogai, S., Koyama, M., 1989. Compositional change of settling particles with water depth in the Japan Sea. Mar. Chem. 27, 61–78.

Maiya, S., Saito, T., Sato, T., 1976. Late Cenozoic planktonic foraminiferal biostratigraphy of northwest Pacific sedimentary sequences. In: Takayanagi, Y., Saito, T. (Eds.), Progress in Micropaleontology. Micropaleontology Press, New York, pp. 295–422.

Mizuno, K., White, W.B., 1983. Annual and interannual variability in the Kuroshio Current System. J. Phys. Oceanogr. 13, 1847–1867.

Mortlock, R.A., Froelich, P.N., 1989. A simple method for the rapid determination of biogenic opal in pelagic marine sediments. Deep Sea Res. 36, 1415–1426.

Müller, P.J., 1977. C/N ratios in Pacific deep-sea sediments: Effect of inorganic ammonium and organic nitrogen compounds sorbed by clays. Geochim. Cosmochim. Acta 41, 765–776.

Müller, P.J., Suess, E., 1979. Productivity, sedimentation rate, and sedimentary organic matter in the oceans – I. Organic carbon preservation. Deep Sea Res. 26A, 1347–1362.

Nakanishi, M., Tamaki, K., Kobayashi, K., 1989. Mesozoic magnetic anomaly lineations and seafloor spreading history of the Northwestern Pacific. J. Geophys. Res. 94, 15437–15462.

Naraoka, H., Ishiwatari, R., 2000. Molecular and isotopic abundances of long-chain n-fatty acids in open marine sediments of the western North Pacific. Chem. Geol. 165, 23–36.

Navy Aerosol Analysis and Prediction System, http://www.nrlmry.navy.mil/aerosol/.

Okamoto, T. Matsumoto, E., Kawahata, H., 2002. Fluctuation of eolian dust flux estimated from cores retrieved from North Pacific during the last 200 kyr. Quat. Res. 41, 35–44 (in Japanese).

Ohkushi, K., Thomas, E., Kawahata, H., 2000. Abyssal benthic foraminifera from the northwestern Pacific (Shatsky Rise) during the last 298 kyr. Mar. Micropaleontol. 38, 119–147.

Prospero, J.M., Glaccum, R.A., Nees, R.T., 1981. Atmospheric transport of soil dust from Africa to South America. Nature 289, 570–572.

Rühlemann, C., Müller, P.J., Schneider, R.R., 1999. Organic carbon and carbonate as productivity proxies: examples from high and low productivity areas of the Tropical Atlan-

tic. In: Fisher, G., Wefer, G. (Eds.), Use of Proxies in Paleoceanography: Examples from the South Atlantic. Springer-Verlag, Berlin, pp. 315–344.

Sancetta, C., Silvestir, S.M., 1986. Pliocene-Pleistocene evolution of the north ocean-atmosphere system, interpreted from fossil diatoms. Paleoceanography 1, 163–180.

Sarnthein, M., Tetzlaff, G., Koopman, B., Wolter, K., Pflaumann, U., 1981. Glacial and interglacial wind regimes over the eastern subtropical Atlantic and north-west Africa. Nature 293, 193–196.

Sarnthein, M., Thiede, J., Pflaumann, U., Erlenkeuser, H., Fütterer, D.K., Koopmann, B., Lange, H., Seibold, E., 1982. Atmospheric and oceanic circulation patterns off Northwest Africa during the past 25 million years. In: Rad Hinz, U., Sarntherin, M., Seibold, E. (Eds.), Geology of the Northwest African Continental Margin. Springer-Verlag, Berlin, pp. 545–604.

Sarnthein, M., Winn, K., Duplessy, J.-C., Fontugne, M.R., 1988. Global variations of surface ocean productivity in low and mid latitude: influence on CO_2 reservoirs of the deep ocean and atmosphere during the last 21,000 years. Paleoceanography 3, 361–399.

Sarnthein, M., Pflaumann, U., Ross, R., Tiedemann, R., Winn, K., 1992. Transfer function to reconstruct ocean paleoproductivity: A comparison, In: Summerhayes, C.P., Prell, W.L., Emeis, K.-C. (Eds.), Upwelling Systems, Evolution since the early Miocene. Geol. Soc. Spec. Publ. 64, pp. 411–427..

Shaffer, G., 1993. Effects of the marine biota on global carbon cycling. In: Heiman, M. (Ed.), The Global Carbon Cycle. Springer-Verlag, Berlin, NATO ASI Series vol. I 15, pp. 431–455.

Sharma, P., Mahannah, R., Moore, W.S., Ku, T.L., Southon, J.R., 1987. Transport of ^{10}Be and ^{9}Be. Earth Planet. Sci. Lett. 86, 69–76.

Sharma, P., Church, T.M., Bernat, M., 1989. Use of cosmogenic ^{10}Be and ^{26}Al in phillipsite for the dating of marine sediments in the south Pacific Ocean. Chem. Geol. 73, 279–288.

Southon, J.R., Ku, T.L., Nelson, D.E., Reyss, J.L., Duplessy, J.C., Vogel, J.S., 1987. ^{10}Be in a deep sea core: implications regarding ^{10}Be production changes over the past 420 ka. Earth Planet. Sci. Lett. 85, 356–364.

Stein, R., 1986. Surface-water paleoproductivity as inferred from sediments deposited in oxic and anoxic deep water. SCOPE/UNEP Sonderband 60, 55–70.

Stevenson, F.J., Chen, C.N., 1972. Organic geochemistry of the Argentine Basin sediments: Carbon-nitrogenic compounds sorbed by clays. Geochim. Cosmochim. Acta 36, 653–671.

Stommel, H., Yoshida, K., 1972. Kuroshio, Physical Aspects of the Japan Current. University of Washington Press, Seattle, WA, 517 pp.

Taylor, S.R., McLennan, S.M., McCulloch, M.T., 1983. Geochemistry of loess, continental crustal composition and crustal model ages. Geochim. Cosmochim. Acta 47, 1897–1905.

Taylor, S.R., McLennan, S.M., 1985. The Continental Crust: Its Composition and Evolution. Blackwell, Oxford, 312 pp.

Thompson, P.R., Shackleton, N.J., 1980. North Pacific palaeoceanography late Quaternary coiling variations of planktonic foraminifer *Neogloboquadrina pachyderma*. Nature 287, 829–833.

Thompson, P.R., 1981. Planktonic foraminifera in the western north Pacific during the past 150,000 yeas: Comparison of modern and fossil assemblages. Palaeogeogr. Palaeoclimatol. Palaeoecol. 35, 241–279.

Thunell, R.C., Mortyn, P.G., 1995. Glacial climate instability in the Northeast Pacific Ocean. Nature 376, 504–506.

Tomczak, M., Godfrey, J.S., 1994. Regional Oceanography: An Introduction. Pergamon, Oxford, 422 pp.

Tsunogai, S., Uematsu, M., Noriki, S., Tanaka, N., Yamada, M., 1982. Sediment trap experiment in the northern North Pacific: undulation of settling particles. Geochem. J. 16, 129–147.

Turekian, K.K., 1964. The marine geochemistry of strontium. Geochim. Cosmochim. Acta 28, 1479–1496.

Windom, H.L., 1975. Eolian contributions to marine sediments. J. Sediment. Petrol. 45, 520–529.